Explicit kinematic-based control allocation for a four-degree-of-freedom redundant radar antenna drive system in target tracking

Le Tran Thang, Dang Nam Kien*

Control, Automation in Production and Improvement of Technology Institute/Academy of Military Science and Technology, 89B Ly Nam De, Hoan Kiem, Hanoi, Vietnam.
*Corresponding author: dangnamkien@gmail.com
Received 27 Jan. 2026; Revised 26 Mar. 2026; Accepted 11 May 2026; Published 25May 2026.
DOI: https://doi.org/10.54939/1859-1043.j.mst.111.2026.22-30

ABSTRACT

The control of a 4-degree-of-freedom (4-DOF) serial manipulator is a key research area in industrial robotics, particularly when the system exhibits actuation redundancy or demands high performance and precision. Handling actuation redundancy and control allocation plays a crucial role in ensuring operational flexibility, dynamic stability, while optimizing criteria such as energy consumption, torque, or obstacle avoidance. Modern research has developed diverse strategies, ranging from traditional optimization-based methods to intelligent techniques integrating deep learning and adaptive control. However, for systems applied in military fields such as radar gimbals, explicit techniques are often prioritized for their simplicity and high reliability. This paper presents an explicit control allocation method for a 4-DOF radar gimbal that effectively resolves practical application-oriented constraints. Accordingly, the naturally incorporated kinematic constraints lead to a control allocation process that aligns with the radar gimbal's operational conditions.

Keywords: Redundant manipulator; 4 degrees of freedom; Control allocation; Target-tracking radar; Hierarchical control.

1. INTRODUCTION

Redundant serial manipulators are robotic systems that possess more degrees of freedom (DOF) than are necessary to perform a specific task [1-3]. This provides significant flexibility, allowing the robot to execute primary tasks in the task space while simultaneously optimizing secondary objectives in the joint space [4-6]. The concept of null-space is central to this capability [5, 7]. By definition, the null-space of the Jacobian matrix contains joint velocities that do not affect the velocity of the end-effector [7]. This enables the robot to perform self-motion to achieve auxiliary goals without interrupting the primary task [7-9].

Traditional studies on explicit redundancy resolution methods for serial manipulators often rely on pseudoinverse-based solutions with null-space projection. Starting from the initial idea of static null-space velocity, some research has particularly focused on making the null-space velocity dynamic [4, 8-10], because with a static null-space, achieving two crucial objectives in target tracking control (both disturbance rejection and stabilizing the line-of-sight, LOS) is not feasible. In these approaches, the authors introduce supplementary dynamics for this null-space portion, transforming it from a strongly forced system into an extended second-order linear system. Here, two important components of the system can have their spectra separated: the LOS changes rapidly while the null-space changes slowly, primarily handling long-term drift.

With a 4-DOF pan-tilt-tilt-pan radar platform, which consists of two main parts: a base section which is a very large and heavy pan-tilt system, and a reflector mirror mounted on a smaller, much lighter tilt-pan mechanism. Consequently, the radar platform's actuator mechanism is redundant for the target tracking control problem (because in practice, only 2 DOF in pan and tilt are needed to track a target). For simple and efficient operation, the fundamental principle during radar target tracking practice is to promptly return the mirror's tilt-pan system to its origin (zero position),

while primarily using the base pan-tilt system to maintain the LOS and track the target. Thus, a redundancy resolution and null-space problem is formed: the primary objective of maintaining the LOS must be sustained, while gradual adjustments in the null-space are made to steer the mirror's angles back to the origin. However, traditional solutions based on the pseudoinverse matrix and its improvements have not been fully effective when applied to the operational principle of this radar platform, because in practice, achieving both objectives within a short time is quite challenging.

To address this issue, this paper presents a dual-loop control method. The outer loop uses a proportional controller to generate desired derivative values, while the inner loop incorporates distinct null-space dynamics specifically for the two tilt-pan joints of the reflector mirror. This allows the reflector mirror to be controlled to converge to the origin according to the desired null-space dynamics.

2. METHODOLOGY

2.1. Forward kinematics of the 4-degree-of-freedom radar platform structure

The radar platform is formed by a 4-degree-of-freedom structure comprising four serial rotary joints, where the base section consists of two pan-tilt joints and the mirror section consists of two tilt-pan joints. Thus, to determine the forward kinematics of the system, coordinate frames (CF) need to be established as shown in Figure 1, including:

(w) Fixed world CF;
(b) Body CF attached at the base of the radar platform;
(p) CF attached at the tilt axis of the radar platform;
(e) CF attached at the tilt axis of the mirror;
(k) CF attached at the pan axis of the mirror.

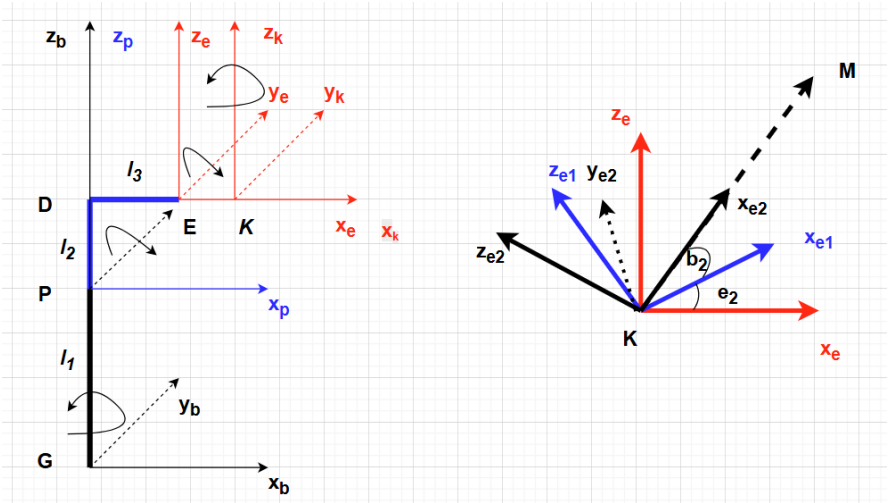

Figure 1. *The kinematic structure of the 4-DOF radar platform.*

Assuming point M is the target coordinate that needs to be tracked, at a relatively far distance (with a range d from 1 km to 11 km), and point K is the endpoint of the radar reflector mechanism, the vector $\overrightarrow{KM}$ can be considered as the line-of-sight vector to the target.

In the coordinate frame (k), the vector $\overrightarrow{KM}$ is the result of all rotations from the four axes, and in the coordinate frame (k), $\overrightarrow{KM^k} = [d, 0, 0]^T$. Therefore, it is necessary to transform $\overrightarrow{KM}$ into the coordinate frame (e) (using the rotation matrices):

$$\overrightarrow{KM}^e = d * \mathbf{R}_{\mathbf{b_2}} * \begin{bmatrix} 1 \\ 0 \\ 0 \end{bmatrix} \tag{1}$$

In coordinate frame (p):

$$\overrightarrow{KM}^{p} = d * \mathbf{R_{e_2}} * \mathbf{R_{b_2}} * \begin{bmatrix}1\\0\\0\end{bmatrix} \tag{2}$$

In coordinate frame (b):

$$\overrightarrow{KM}^{b} = d * \mathbf{R_{e_1}} * \mathbf{R_{e_2}} * \mathbf{R_{b_2}} * \begin{bmatrix}1\\0\\0\end{bmatrix} \tag{3}$$

In coordinate frame (w):

$$\overrightarrow{KM}^{w} = d * \mathbf{R_{b_1}} * \mathbf{R_{e_1}} * \mathbf{R_{e_2}} * \mathbf{R_{b_2}} * \begin{bmatrix}1\\0\\0\end{bmatrix} \tag{4}$$

Therefore, since all rotation matrices are normalized, the normalized line-of-sight vector is:

$$\overrightarrow{KM_o}^{w} = \mathbf{R_{b_1}} * \mathbf{R_{e_1}} * \mathbf{R_{e_2}} * \mathbf{R_{b_2}} * \begin{bmatrix}1\\0\\0\end{bmatrix} = \begin{bmatrix}\cos b_2 \cos b_1 \cos(e_1+e_2) - \sin b_1 \sin\ b_2\\ \cos b_2 \sin b_1 \cos(e_1+e_2) + \cos b_1 \sin\ b_2\\ -\cos b_2 \sin(e_1+e_2)\end{bmatrix} \tag{5}$$

When the vector $\overrightarrow{KM_o}$ is projected onto the Oxy and Oxz planes, two angles β and ϵ are obtained. In the spherical coordinate system, these angles correspond to the azimuth and elevation angles, respectively. Therefore:

$$\overrightarrow{KM_o}^{w} = \begin{bmatrix}\cos(\beta)\cos(\epsilon)\\ \sin(\beta)\cos(\epsilon)\\ \sin(\epsilon)\end{bmatrix} \tag{6}$$

Therefore, since the angle $\epsilon \in [0^0; 85^0]$ (and thus $\cos(\epsilon) > 0$), it can be calculated directly as:

$$\epsilon = \operatorname{asin}(\overrightarrow{KM_o}^{w}[2]) \tag{7a}$$

$$\beta = \operatorname{atan}2(\overrightarrow{KM_o}^{w}[1], \overrightarrow{KM_o}^{w}[0]) \tag{7b}$$

(5) can be transformed to:

$$\overrightarrow{KM_o}^{w} = \begin{bmatrix}\cos b_2 \cos b_1 \cos(e_1+e_2) - \sin b_1 \sin b_2 \cos(e_1+e_2)\\ \cos b_2 \sin b_1 \cos(e_1+e_2) + \cos b_1 \sin b_2 \cos(e_1+e_2)\\ -\sin(e_1+e_2)\end{bmatrix} + \begin{bmatrix}\sin b_1 \sin b_2 \cos(e_1+e_2) - \sin b_1 \sin\ b_2\\ -\cos b_1 \sin b_2 \cos(e_1+e_2) + \cos b_1 \sin\ b_2\\ +\sin(e_1+e_2) - \cos b_2 \sin(e_1+e_2)\end{bmatrix} =$$

$$\begin{bmatrix}\cos(b_1+b_2)\cos(e_1+e_2)\\ \sin(b_1+b_2)\cos(e_1+e_2)\\ -\sin(e_1+e_2)\end{bmatrix} + \begin{bmatrix}\sin b_1 \sin b_2\,[\cos(e_1+e_2)-1]\\ -\cos b_1 \sin b_2\,[\cos(e_1+e_2)-1]\\ \sin(e_1+e_2)\,[1-\cos b_2]\end{bmatrix} \tag{8}$$

When the angles e_2 and b_2 are small, an approximate calculation can be made:

$$\sin b_2 = 0; \cos b_2 = 1 \tag{9}$$

Substitute to (8):

$$\overrightarrow{KM_o}^{w} \approx \begin{bmatrix}\cos(b_1+b_2)\cos(e_1+e_2)\\ \sin(b_1+b_2)\cos(e_1+e_2)\\ -\sin(e_1+e_2)\end{bmatrix} \tag{10}$$

Thus, it can be understood that the equivalent angles can be determined as the algebraic sum of the angles about the same rotational axes:

$$\epsilon = -e_1 - e_2 \tag{11a}$$

$$\beta = b_1 + b_2 \tag{11b}$$

The difference in sign is mainly due to the choice of different coordinate systems.

2.2. Dynamic null-space embedded dual-loop control

For the outer control loop handling target line-of-sight, a conventional proportional control law is used. Accordingly, the outer loop controller needs to determine an intermediate required value:

$$\dot{\mathbf{y}}_* = \dot{\mathbf{y}}_\mathbf{d} - K\mathbf{e} \text{ where } \mathbf{e} = \mathbf{y} - \mathbf{y}_\mathbf{d} \tag{12}$$

Where: $\mathbf{y} = [\epsilon\ \beta]^T$; $\mathbf{y_d}$ is desired value.

This intermediate value $\dot{y}_*$ ensures the ability to track the target line-of-sight. Since the focus of this study is not on this control loop, a simple controller is chosen. The main task lies in the inner loop, where this intermediate value serves as the basis for determining control allocations within the null-space dynamics, aiming to adjust the tilt-pan mirror toward its origin. Accordingly, by dividing the system into two components—the base and the mirror—we have the following distinct states:

$$\mathbf{q_b} = \begin{bmatrix} b_1 \\ e_1 \end{bmatrix};\ \mathbf{q_r} = \begin{bmatrix} b_2 \\ e_2 \end{bmatrix} \tag{13}$$

Then, from (11a), (11b) and (13):

$$\mathbf{y} \approx \mathbf{q_b} + \mathbf{q_r} \tag{14}$$

Then, to ensure that $\mathbf{q_r}$ converges to $\begin{bmatrix} 0 \\ 0 \end{bmatrix}$, an inner control loop embeds a null-space dynamics based on the intermediate value $\dot{y}_*$:

$$\begin{cases} \dot{\mathbf{q}}_\mathbf{r} = -\begin{bmatrix} \lambda & 0 \\ 0 & \lambda \end{bmatrix} \mathbf{q_r} + \begin{bmatrix} \zeta & 0 \\ 0 & \zeta \end{bmatrix} \dot{\mathbf{y}}_* & \text{(15a)} \\ \dot{\mathbf{q}}_\mathbf{b} = \dot{\mathbf{y}}_* - \dot{\mathbf{q}}_\mathbf{r} & \text{(15b)} \end{cases}$$

Here, the value of λ is very large compared to ζ to ensure that the null-space dynamics are fast relative to the target line-of-sight tracking. This is because in practice, when the tracking error is small, according to (12), $\dot{\mathbf{y}}_* \to \dot{\mathbf{y}}_\mathbf{d}$, while $\dot{\mathbf{y}}_\mathbf{d}$ is bounded, typically limited by the actuator's capability. Therefore, equation (15a) can be approximately rewritten as:

$$\dot{\mathbf{q}}_\mathbf{r} \approx -\begin{bmatrix} \lambda & 0 \\ 0 & \lambda \end{bmatrix} \mathbf{q_r} \tag{16}$$

The solution to this equation takes the form:

$$\mathbf{q_r}(t) = \mathbf{q_r}(0)e^{-\lambda t} \tag{17}$$

Thus, if $t \to \infty$, then $\mathbf{q_r} \to 0$, meaning the system achieves the required null-space dynamics.

Meanwhile, equation (15b) ensures that the target line-of-sight is consistently maintained. It is a consequence of equation (14).

2.3. Disturbances and model errors

In practice, radar operation is always subject to noise, as it is very difficult for a radar to measure the exact elevation and azimuth angles. Angular noise, jitter, and filtering errors always exist. Consequently, the actual measured error is:

$$\mathbf{e} = (\mathbf{y} + \mathbf{n_y}) - \mathbf{y_d} \tag{18}$$

Where:

$$\mathbf{n_y} = \begin{bmatrix} n_{az} \\ n_{el} \end{bmatrix} \tag{19}$$

Where each channel component has the form:

$$n_{y_i}(s) = \frac{\omega_n}{s+\omega_n}\omega(t) \tag{20}$$

where *ω(t)* is Gaussian white noise, and ω_n is the cutoff frequency of the filter.

Additionally, the kinematic model always contains mapping errors from velocity to actual angle. Therefore:

$$\dot{\mathbf{q}}_{\mathbf{real}} = (1+\Delta)\dot{\mathbf{q}}_{\mathbf{cmd}} \tag{21}$$

Where Δ is an uncertain parameter describing the percentage deviation between the commanded angular rate and the actual angular rate. This value is typically bounded; for the 4-DOF radar platform, Δ ∈ [-0.2, +0.2].

3. SIMULATION RESULTS AND DISCUSSION

3.1. Simulation scenario

The required trajectory is given by specific functions for each axis:

$$\begin{aligned} y_{bd} &= \frac{\pi}{180} * t \\ y_{ed} &= \left(15 * \frac{\pi}{180}\right) * \sin(t) \end{aligned} \tag{22}$$

Where: y_{bd} is the desired azimuth angle, y_{ed} is desired elevation angle.

System parameters:

$$\begin{aligned} K &= 10 \\ \lambda &= 8 \\ \zeta &= 0.2 \\ \omega_n &= 2 * \pi * 10 \end{aligned} \tag{23}$$

In addition to the dynamic null-space embedded dual-loop control (Dynamic NEDL) system, the pseudoinverse matrix method is also considered and compared in two cases: static pseudoinverse-based redundancy resolution (Static PRR) and dynamic pseudoinverse-based redundancy resolution (Dynamic PRR). Accordingly, for the case using the pseudoinverse matrix, the velocity calculation expression is given by:

$$\dot{\mathbf{q}} = \mathbf{J}^{+}\dot{\mathbf{y}}_{*} + (\mathbf{I} - \mathbf{J}^{+}\mathbf{J})\mathbf{z} \tag{24}$$

Where **J** is the Jacobian matrix mapping from the state space to the operational space, with dimensions 2x4; $\mathbf{J}^{+}$ is the pseudoinverse of **J**, with dimensions 4x2; **z** is given by:

$$\mathbf{z} = [0, 0, -k_r e_2, -k_r b_2]^T \tag{25}$$

Equation (25) represents the case of static null-space with a constant coefficient k_r. To modify it for dynamic null-space control, a null-space memory needs to be added:

$$\dot{\boldsymbol{\eta}} = -k_\eta \boldsymbol{\eta} + \mathbf{q_r} \tag{26}$$

Anh chose:

$$\mathbf{z} = -k_r \boldsymbol{\eta} \tag{27}$$

Then, we choose the coefficients as follows (based on the fact that null-space needs to be slower than outer loop):

$$\begin{aligned} k_r &= 1.2 \\ k_\eta &= 8 \end{aligned} \tag{28}$$

3.2. Simulation results

The simulation results are shown in Figures 2 to 7, where Figures 2 and 3 illustrate the target tracking errors of the radar platform for all three methods.

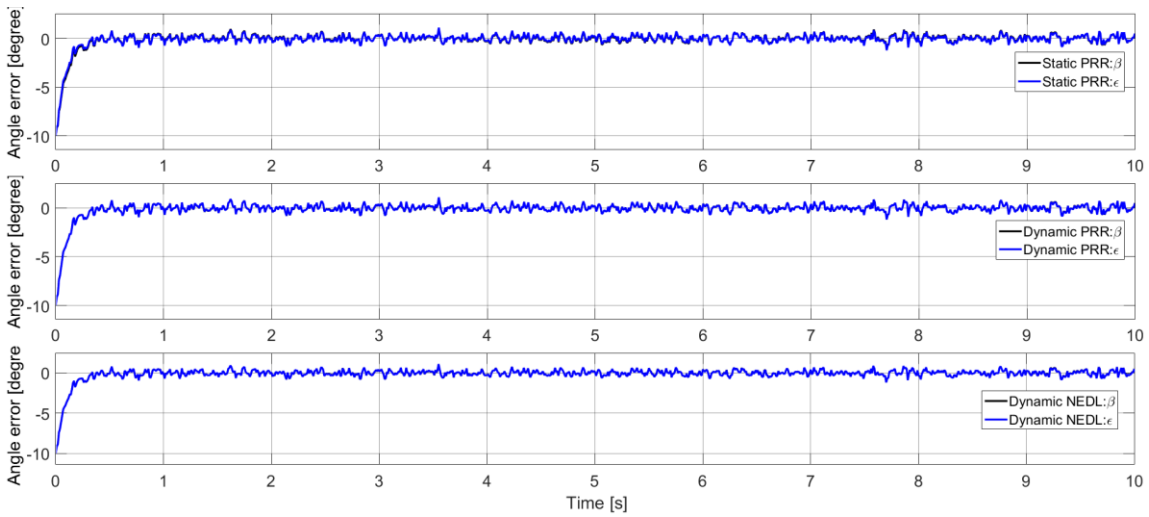

Figure 2. *Elevation and azimuth tracking angle errors of the three methods.*

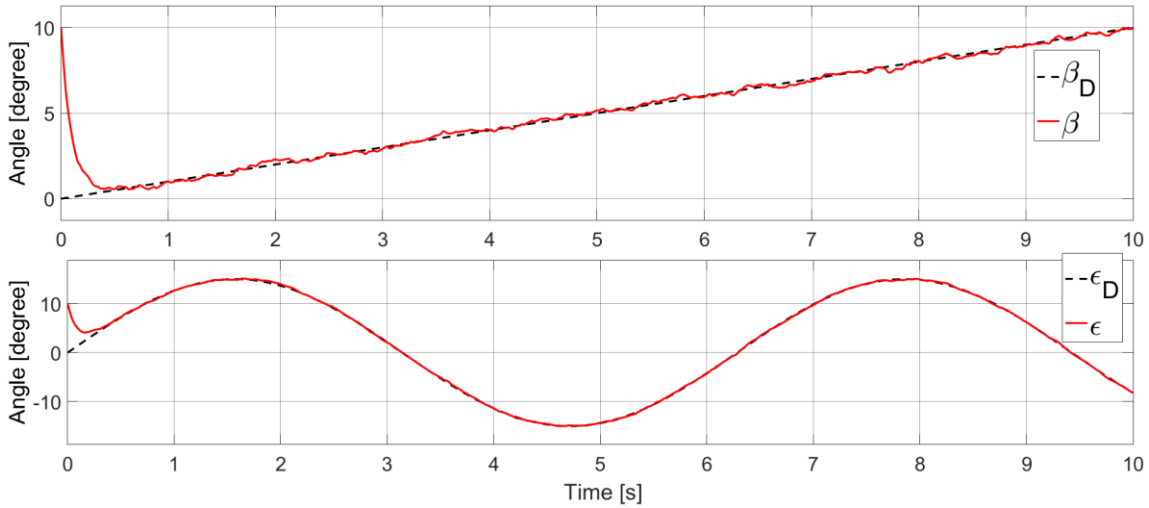

Figure 3. *Elevation and azimuth angle values of the three methods compared to the setpoint values.*

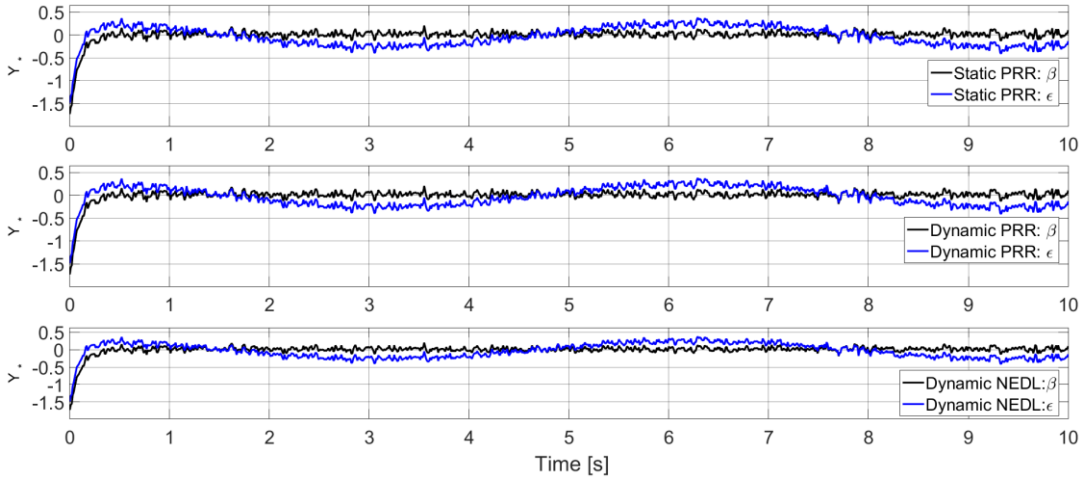

Figure 4. *The outer-loop control signal $\dot{y}_*$ for the three methods.*

Based on the results shown in Figures 2 and 3, it can be observed that all three methods ensure excellent target trajectory tracking performance. Embedding null-space dynamics or using the pseudoinverse matrix method hardly affects the radar's target tracking task.

Figure 4 shows the outer-loop control signal $\dot{y}_*$ for the three methods, with the results indicating that all three have similar control signals, demonstrating the objectivity of the research findings.

Figures 5 to 7 illustrate the angles of the radar platform when using the three methods for target tracking. The focus is on the reflector mirror angles, as the primary task of the redundancy resolution control problem is to utilize null-space dynamics to bring the reflector mirror back to the origin while tracking the target. It can be observed that the Dynamic PRR method can pull the reflector mirror to a vicinity around the origin, but with a relatively large amplitude, where the mirror's elevation angle falls outside the range $[-5^0, 5^0]$ degrees. The azimuth angle converges quite well to the origin; however, the convergence time remains long, approximately 10 seconds.

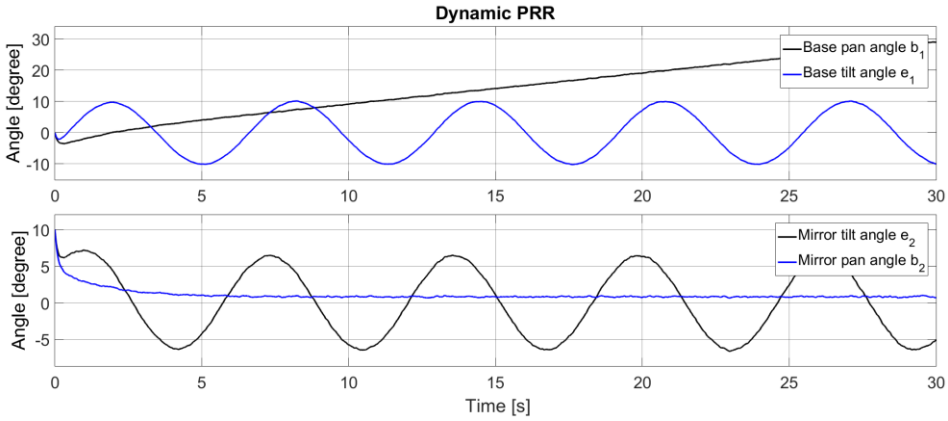

Figure 5. *The angles of the radar platform when using Dynamic PRR.*

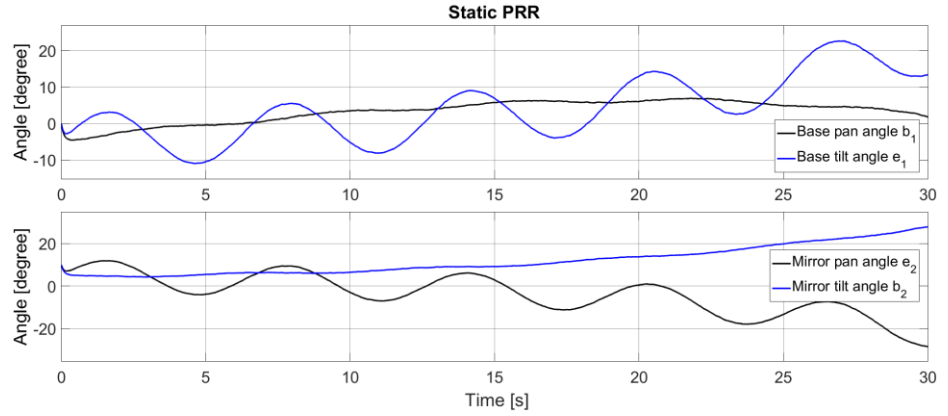

Figure 6. *The angles of the radar platform when using Static PRR.*

Figure 6 shows the results of Static PRR, where it is evident that the reflector mirror angles do not converge to the origin at all. While the azimuth angle gradually drifts away, the mirror's elevation angle oscillates and slowly decreases. Consequently, after 30 seconds, these angles are far from the origin. Thus, for the Static PRR case, the system's operational objective is not achieved.

Figure 7 presents the results of the Dynamic NEDL method. It can be immediately seen that in this case, the reflector mirror angles converge rapidly to the origin and then oscillate with a very small amplitude. For the mirror's azimuth angle, this amplitude is less than $[-0.5^0, 0.5^0]$ degrees. Particularly for the mirror's elevation angle, there is almost negligible deviation from the origin.

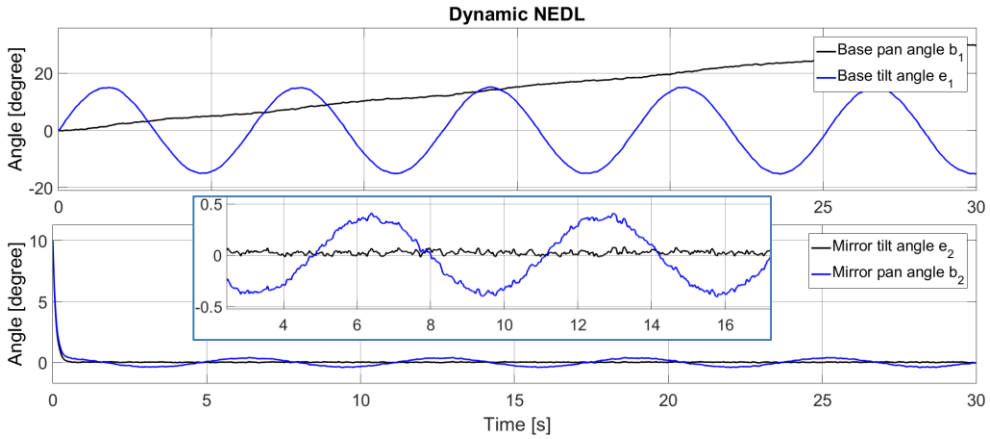

Figure 7. *The angles of the radar platform when using Dynamic NEDL.*

These results are further confirmed in Table 1, which provides a direct comparison of the RMSE for the tracking angle errors of the three methods as well as the deviation from the mirror's origin. It is immediately evident that, while the trajectory tracking errors are nearly equivalent, the deviations from the mirror's origin differ significantly. While Static PRR has average deviations as high as 13.4^0 and 10^0, the deviations for the Dynamic PRR method are 4.69^0 and 1.29^0, respectively—more than halved. Notably, Dynamic NEDL, the proposed method, improves the angular deviation by over 20 times compared to Static PRR, with values of 0.496^0 and 0.407^0, respectively.

Table 1. *Comparisons between three methods.*

	Dynamic NEDL	**Static PRR**	**Dynamic PRR**
RMSE e_{azi} [degree]	0.517	0.511	0.511
RMSE e_{ele} [mdegree	0.506	0.511	0.511
RMSE b_2 [degree]	0.496	13.4	4.69
RMSE e_2 [degree]	0.407	10	1.29

4. CONCLUSIONS

This paper has proposed an explicit, dynamics-based control allocation method for a four-degree-of-freedom redundant radar platform in a target tracking problem. The method utilizes a dual-loop control structure embedded with null-space dynamics, where the tasks of maintaining the line-of-sight (LOS) and adjusting the redundant joints are clearly separated. This allows for control role allocation that aligns with the physical structure and actual operational principles of the radar platform.

Simulation results demonstrate that the proposed Dynamic NEDL method maintains target tracking quality equivalent to pseudoinverse-based methods while clearly outperforming them in null-space control capability. The tilt–pan mirror angles converge rapidly and stably to the origin with very small deviations, whereas Static PRR and Dynamic PRR methods either fail to converge or converge slowly with large oscillation amplitudes. Quantitative RMSE comparisons confirm the superior effectiveness of the proposed method in handling redundancy resolution without compromising the primary task.

From an academic perspective, this research demonstrates an approach to transforming the redundancy resolution problem from algebraic projection to explicit dynamic design, resulting in a control structure that is simple, intuitive, and highly applicable. In the future, this research will be extended towards experimental validation on a real radar system, as well as the integration of

advanced control and estimation techniques to enhance the system's robustness against disturbances and uncertainties.

REFERENCES

[1]. Ramos M. C., & Koivo A. J. *"Fuzzy logic based optimization for manipulators"*. Proceedings 2000 ICRA. Millennium Conference. IEEE International Conference on Robotics and Automation, Symposia Proceedings (Cat. No.00CH37065), Vol. 3, pp. 2289–2294, (2000). DOI: 10.1109/robot.2000.845285

[2]. Ghosal A. *"Resolution of redundancy in robots and in a human arm"*. Mechanism and Machine Theory, 125, pp. 1–11, (2018). DOI: 10.1016/j.mechmachtheory.2017.12.008

[3]. Shen Y., Jia Q., Huang Z., Wang R., Fei J., & Chen G. *"Reinforcement Learning-Based Reactive Obstacle Avoidance Method for Redundant Manipulators"*. Entropy, 24, (2), 279, (2022). DOI: 10.3390/e24020279

[4]. Woliński Ł., & Wojtyra M. *"An inverse kinematics solution with trajectory scaling for redundant manipulators"*. Mechanism and Machine Theory, 189, 105493, (2023). DOI: 10.1016/j.mechmachtheory.2023.105493

[5]. Rahmouni M. A., Bearee R., Grossard M., & Lucet E. *"Vibration reduction control for redundant flexible robot manipulators"*. IFAC-PapersOnLine, 53, (2), pp. 16301–16306, (2020). DOI: 10.1016/j.ifacol.2020.12.1422

[6]. Verotti M., Masarati P., Morandini M., & Belfiore N. P. *"Active isotropic compliance in redundant manipulators"*. Multibody System Dynamics, 48, (3), pp. 263–288, (2020). DOI: 10.1007/s11044-020-09724-9

[7]. Kim S., Yun S., & Shin D. *"Numerical Quantification of Controllability in the Null Space for Redundant Manipulators"*. Applied Sciences, 11, (13), 6190, (2021). DOI: 10.3390/app11136190

[8]. Karami A., Sadeghian H., & Keshmiri M. *"Novel approaches to control multiple tasks in redundant manipulators: stability analysis and performance evaluation"*. Advanced Robotics, 32, (6), pp. 332–347, (2018). DOI: 10.1080/01691864.2018.1442744

[9]. Woolfrey J., Lu W., & Liu D. *"A Control Method for Joint Torque Minimization of Redundant Manipulators Handling Large External Forces"*. Journal of Intelligent & Robotic Systems, 93, (1), pp. 163–175, (2019). DOI: 10.1007/s10846-018-0964-8

[10]. Oda N., Murakami T., & Ohnishi K. *"Robust motion control in redundant motion systems"*. AMC'98 Coimbra. 1998 5th International Workshop on Advanced Motion Control. Proceedings (Cat. No.98TH8354), pp. 642–647, (1998). DOI: 10.1109/amc.1998.743484

TÓM TẮT

Phân bổ điều khiển tường minh bằng động học cho bệ radar dư dẫn động bốn bậc tự do bám mục tiêu

Bài toán điều khiển tay máy nối tiếp 4 bậc tự do (4-DOF) là một lĩnh vực nghiên cứu trọng tâm trong robot công nghiệp, đặc biệt khi hệ thống thể hiện tính dư dẫn động hoặc yêu cầu cao về hiệu suất và độ chính xác. Việc xử lý dư dẫn động (redundancy resolution) và phân bổ điều khiển (control allocation) đóng vai trò then chốt trong việc đảm bảo khả năng làm việc linh hoạt, ổn định động học, đồng thời tối ưu hóa các tiêu chí như năng lượng, mô-men lực, hay tránh vật cản. Các nghiên cứu hiện đại đã phát triển nhiều chiến lược đa dạng, từ phương pháp truyền thống dựa trên tối ưu hóa đến các kỹ thuật thông minh tích hợp học sâu và điều khiển thích nghi, tuy nhiên với các hệ thống được ứng dụng trong lĩnh vực quân sự như bệ radar các kỹ thuật tường minh vẫn được ưu tiên hơn vì sự đơn giản và độ tin cậy cao. Bài báo này trình bày một phương pháp phân bổ điều khiển bệ radar bốn bậc tự do một cách tường minh mà giải quyết hiệu quả các ràng buộc có tính ứng dụng cao trong thực tế sử dụng. Theo đó ràng buộc động học được thêm vào tự nhiên sẽ kéo theo quá trình phân bổ điều khiển phù hợp với điều kiện sử dụng của bệ radar.

Từ khoá: Robot dư dẫn động; 4 bậc tự do; Phân bổ điều khiển; Radar bám mục tiêu; Điều khiển phân cấp.